SATURATION CARRYING CAPACITY OF GAS AND FLOW REGIMES IN CFB

DINGLONG BAI AND KUNIO KATO*
Department of Biological and Chemical Engineering Gunma University, Kiryu, Gunma 376

Keywords: Saturation Carrying Capacity, Solid Holdup, Flow Regime, Circulating Fluidized Beds, Pneumatic Transport

This paper presents a generalized approach to the saturation carrying capacity of *gas*, G_s*, in high-velocity fluidized beds. Starting from discussion of the variation of solid holdup in the dense region of circulating fluidized beds (CFBs) with the solid circulation rate, we defined the saturation carrying capacity of *gas*, G_s*, as the solid circulation rate at which a maximum achievable or saturation solids concentration at the dense region of the CFB starts to be reached. It has been experimentally demonstrated that above G_s*, solid concentrations in the dense region are really independent of changes in the solid circulation rate, the riser diameter, solids feeding system and the solids inventory, and a characteristic S-shaped axial solid holdup distribution would be observed. Based on this physical phenomenon, the saturation carrying capacity of gas was determined as functions of gas velocity and gas-solid properties, and a generalized correlation was therefore proposed on the basis of collected literature data. Finally, a flow diagram in which the flow conditions for occurring of S-shaped and exponential profiles of solids holdup was presented.

Introduction

As an essential concept for description of hydrodynamic conditions in gas-solids flow systems, the term Saturation Carrying Capacity (SCC) of *gas* is frequently encountered in the literature relating to fast or circulating fluidization (Li et al., 1988, Yerushalmi and Cankurt, 1979), solid transport, as well as the entrainment of solids from a fluidized bed (Wen and Chen, 1982, Zenz and Weil, 1958, Zenz and Othmer, 1960). In the literature, two major different approaches for determining SCC can be identified. From the viewpoint of solids entrainment, the first approach has generally taken the saturation carrying capacity of gas as the entrainment rate above the TDH where it appears constant along the freeboard height. For a pneumatic transport line, it has been found that for a given fluid-solid system there is a maximum attainable solid mass flow rate that can be held in dilute flowing suspension with no axial variation at a given gas velocity. In this case, a slight increase in the solid circulation rate will lead to an axially uniform distribution of solids reflected by a step-wise change in bed voidage or accumulation of particles in the lower part of the riser. This phenomenon has been commonly referred to as choking by many investigators (Wen and Chen, 1982, Zenz and Weil, 1958, Zenz and Othmer, 1960). Accordingly, the second approach determined the SCC as the solid circulation rate at choking condition (Matsen, 1982, Li et al., 1988, Chang and Louge, 1992).

It is clear that there is still a certain amount of confusion surrounding the saturation carrying capacity of gas. For example, a possible variation in solid concentration above TDH with solids circulation rate was not taken into account in the first approach. On the other hand, the data and the reported correlations of SCC by the first approach are hard to extend to high gas velocity operations. For the second approach, the determined SCC probably does not reflect the maximum transport capacity of the flowing gas stream—as noted in many investigations—it just describes the defined choking condition in a transport line. This is mainly because the solid concentration does not reach its saturation value, and it is still plausible to increase the solid concentration, even with increasing solid circulation rate at a given gas velocity. In addition, as pointed out by Yang (1983) and many others, the fact that the effect of pipe diameter plays a significant role in the choking condition appears to contradict the physical interpretation of the SCC. Obviously, it is unlikely that such differing approaches can give consistent results. Therefore, there is a need to clarify the physical mechanism of SCC and to develop a generalized correlation for estimation of SCC.

The purpose of this study is to provide a new perspective based on the existing solids holdup data at the bottom of the riser of circulating fluidized beds, and to propose a more general correlation for the saturation carrying capacity of gas. Finally, a discussion is made for classifying the fast fluidization regime into two regions, a region where solid axial distribution is S-shaped, and a region where solid axial distribution is exponential.

1. Analysis

For a vertical riser in which solids are being

* Received September 5, 1994. Correspondence concerning this article should be addressed to K. Kato.

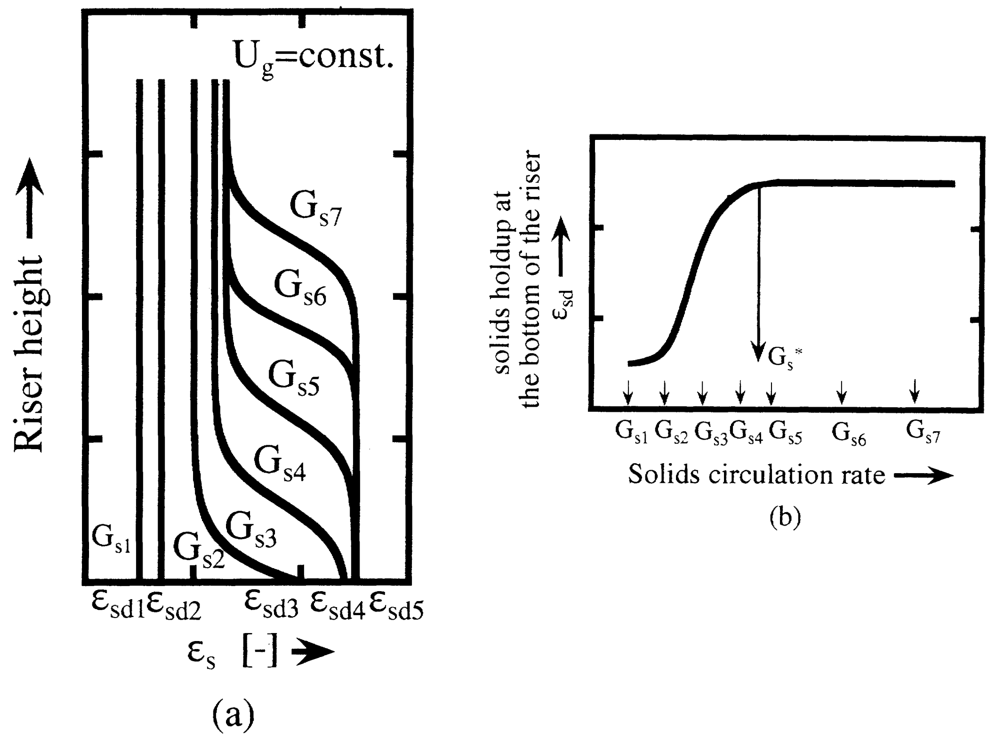

Fig. 1 Typical axial profiles of solid holdup (a) and variation of solid holdup at the bottom of the riser (b) with solid circulation rate for a given gas velocity

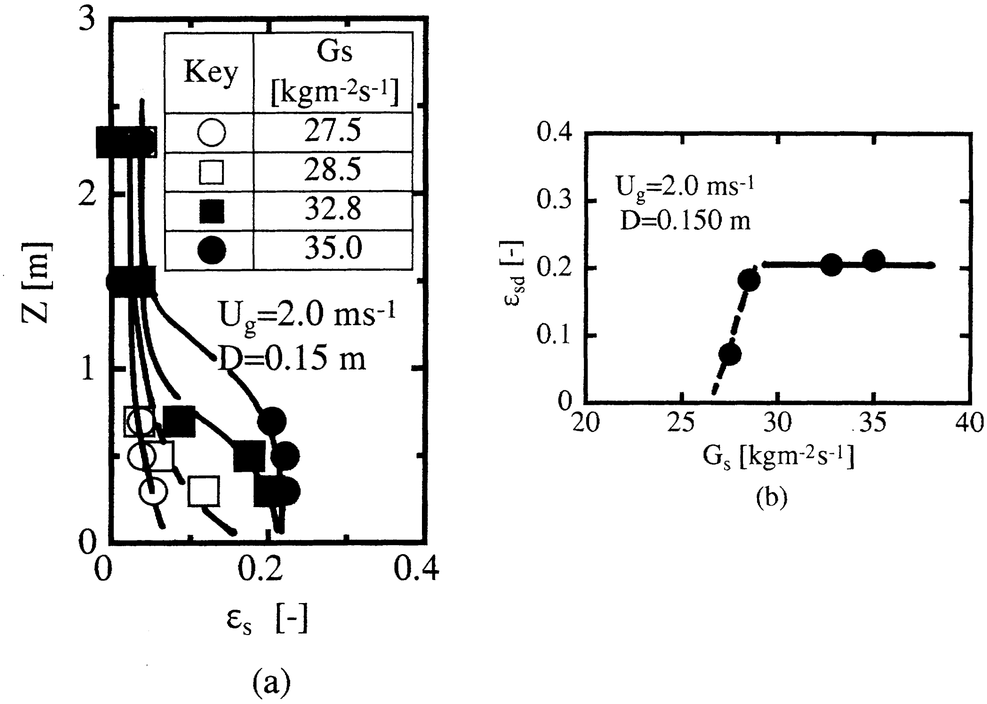

Fig. 2 An example of experimental axial profile of solid holdup (a) and variation of solid holdup at the bottom of the riser (b) with solid circulation rate for a given gas velocity

conveyed upward apparently at a given gas velocity, when the solid circulation rate is gradually increased (achievable by changing the solid inventory thought adjusting the solids control valve), the axial distributions of the solid holdup can be ideally illustrated in **Fig. 1(a)**. This responds to an ideal situation where the riser has a smooth exit at its top and an entrance structure with weak restriction. The corresponding solids holdup at the bottom of the riser is shown in **Fig. 1(b)**. In light of previous extensive experimental observations and the understanding of gas-solids

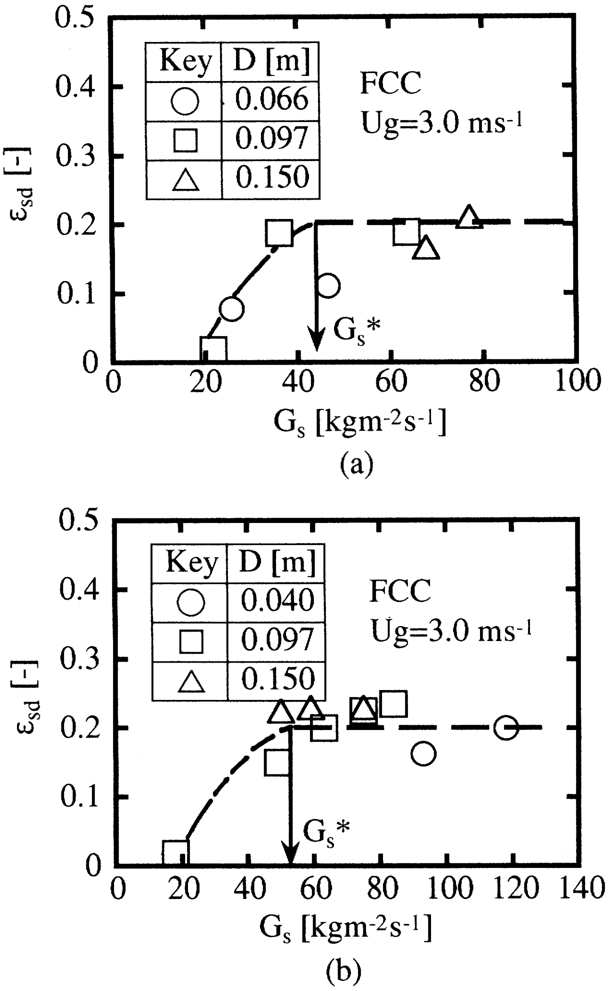

Fig. 3 Variation of solids holdup at dense region with solid circulation rate for different riser diameters. The data shown in (a) and (b) are obtained from Bai and Kato (1994) and Nishino (1990), respectively ($D_s = 0.105$ m)

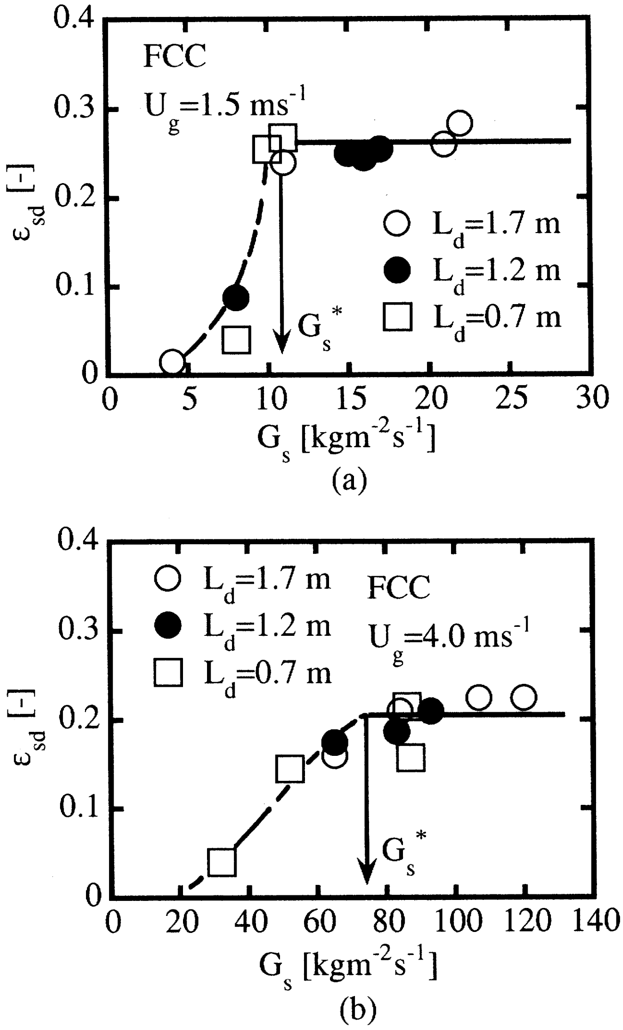

Fig. 4 Variation of solids holdup in dense region with solid circulation rate for different solids inventory. The data are obtained from Nishino (1990) ($D_s = 0.105$ m)

flow, we can describe the above process as follows. At a very low solids rate ($G_s = G_{s1}$, for example), the solids move co-currently upward with the gas. In this case, a much more uniform axial distribution of solids is observable. This flow pattern has been well defined as dilute pneumatic transport, where an increase in the solid circulation rate usually leads to a slight increase in solids holdup ($G_s = G_{s2}$). As the solid circulation rate is further increased ($G_s = G_{s3}$), the solids can no longer be individually suspended in the riser. Consequently, a relatively dense bed forms at the bottom of the riser. In other words, the flow is being translated from a pattern where all particles are traveling upwards with no axial concentration profile of solids to a mode where there is an axial concentration profile of solids. Although many previous works determined the values of SCC based on this criterion, the authors believe that this formation of dense bed or accumulation of particles at the riser bottom is results mainly from enhanced collision and interaction between the solids that slow down the velocity of particles, especially in the lower part of the riser where the particles have not been fully accelerated. Therefore, a stepwise change in bed concentration can not be considered as a feature of saturation carrying capacity. This means that the solid concentration in this case can still increase as the solid circulation rate increases, as shown in Fig. 1(b).

A further increase in the solid circulation rate will result in a steep axial distribution in solid holdup and a continuous increase in solid holdup in the lower region ($G_s = G_{s4}$). However, when the solid circulation rate is increased to a value at which much of the solid begins to accumulate at the bottom of the riser and a typical S-shaped solid holdup distribution starts to form, a maximum achievable solid holdup in the dense region, i.e., a saturation solid concentration, is finally reached. Logically, the solid circulation rate at this point should reflect the maximum transportable capacity of the flow gas stream. Further increasing the solid circulation rate beyond this critical point will have no effect on solid holdup in the dense region (see Fig. 1(b)), it only causes growth of the dense region as the interface between the dense and dilute region rises up the riser ($G_s = G_{s6}$, G_{s7}). If sufficient driving

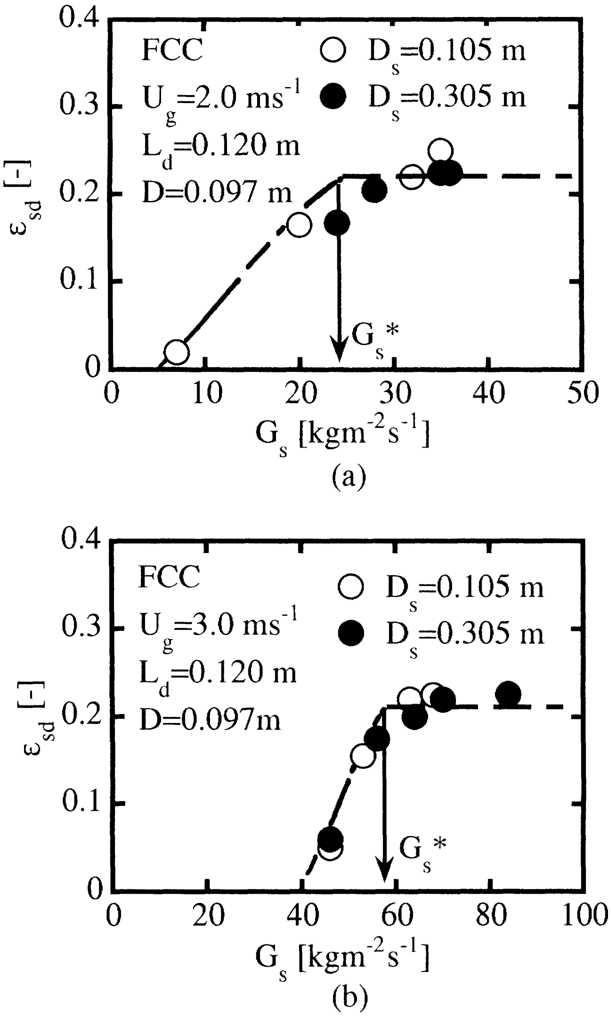

Fig. 5 Variation of solids holdup in dense region with solid circulation rate for two different standpipe diameters. The data are obtained from Nishino (1990)

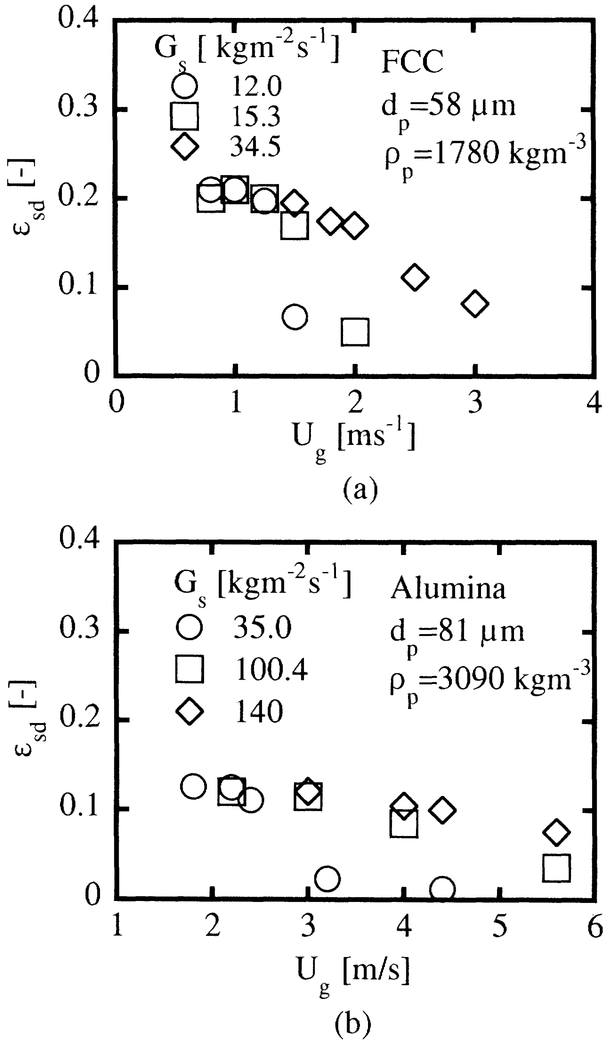

Fig. 6 Variation of solid holdup at dense region with gas velocity. The data are obtained from Li and Kwauk (1980) and Chen *et al.* (1980)

force is available to push the solids into the riser, the dense region may eventually completely fill the riser.

To summarize, by demonstrating the variation of solid holdup in the lower region of the riser versus the solid circulation rate, one can determine the saturation carrying capacity of gas under which the solid holdup achieves saturation independent of solid circulation rate, the geometry of the riser, the solid inventory, or the system configuration. Therefore, the saturation carrying capacity of gas should be determinable by plotting the solid holdup at the bottom of the riser against the solid circulation rate, as shown in Fig. 1(b).

2. Experimental Results

As an example (Bai and Kato, 1994), the experimental axial profile of solid holdup and the variation of solid holdup at the bottom of the riser with the solid circulation rate are given in **Fig. 2**. Clearly, the results indicate that the above analysis is reasonable.

Figure 3 shows the variation of solid holdups at the bottom of the riser with the solid circulation rate for three kinds of riser diameters. The data shown in Figs. 3(a) and 3(b) are obtained from Bai and Kato (1994) and Nishino (1990) in a circulating fluidized bed. For a given operating gas velocity of U_g = 3.0 ms^{-1}, the solids holdup at the bottom of the riser, ε_{sd}, is small and increases significantly with increasing solid circulation rate in the range of low solid circulation rate. When the solid circulation rate is raised up to a critical value, termed G_s* here, ε_{sd} becomes insensitive to change in the solid circulation rate. It is also noted that ε_{sd} appears to be independent of the riser diameter, but may vary with gas velocity when $G_s > G_s$*.

As pointed out in earlier studies (e.g., Weinstein, et al., 1984, Li et al., 1988, Nishino, 1990, Gao, 1990, Kunii and Levenspiel, 1991), solid holdups at the bottom of the riser are indeed independent of solid inventory in cases of co-existence of a lower dense region and an upper dilute region (i.e., $G_s > G_s$*), as shown in **Fig. 4**. This phenomenon has been further confirmed by examining other experimental data reported in the literature (e.g., Li and

Table 1. Summary of the experimental conditions used in the correlation

Investigators	Solids	d_p (μm)	ρ_p (kgm^{-3})	Keys
Nishino (1990)	FCC	69	1690	○
Bai and Kato (1994)	FCC	51.9	1623	□
Yang and Sun (1991)	Silicagel	165	794	◇
	Silicagel	325	794	×
Li and Kwauk (1980)	Alumina	81	3090	+
	Pyrite cinder	56	3050	△
	Iron concentrate	105	4510	●
	FCC	58	1780	■
Yerushalmi and Cankurt (1979)	FCC	49	1070	◆
	HFZ-20	49	1450	▲
Takeuchi et al. (1986)	FCC	57	1080	▼
Gao (1990)	FCC	62	1020	◉
	Silicagel	205	760	⧅
	AN catalyst	82	1780	⊞
Li et al. (1988)	FCC	54	930	▽
Bi et al. (1992)	FCC	65	1510	◐
Ouyang and Potter (1993)	FCC	65	1380	◒
Rhodes and Geldart (1986)	9G	64	1800	◨

* Correspondence concerning this article should be addressed to K. Kato.

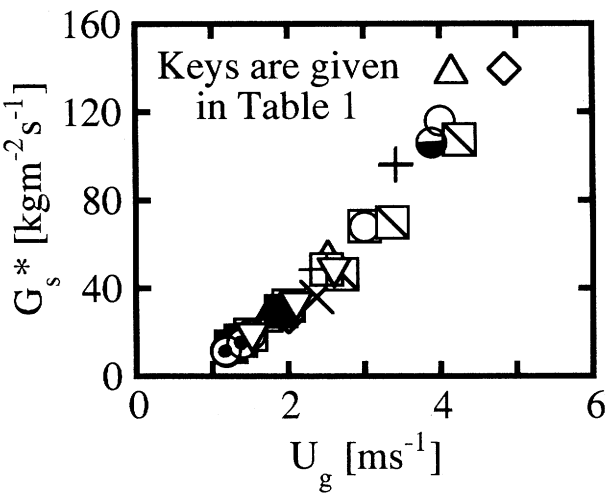

Fig. 7 Gs* as a function of gas velocity for various solid particles

Kwauk, 1980, Yerushalmi and Avidan, 1985, Bi et al., 1989, Yang and Sun, 1991, Bai et al., 1993).

When the riser diameter and the solids inventory are fixed, the solids holdup ε_{sd} is plotted against the solid circulation rate for two kinds of slow bed diameters in **Fig. 5**. As expected, the solid holdup ε_{sd} is almost uninfluenced by slow bed diameter after the saturation state is reached.

Figure 6 represents the results obtained from experimental measurements of Li and Kwauk (1980) and Chen *et al.* (1980). It shows that for a given solid circulation rate, an increase in solid holdup at the bottom of the riser is clearly observed with reducing gas velocity. A point at which ε_{sd} becomes a constant is finally reached when gas velocity is further reduced. Corresponding to this point, the higher the solid circulation rate, the larger the gas velocity. This reflects, as observed earlier, that the saturation carrying capacity of gas increases with gas velocity.

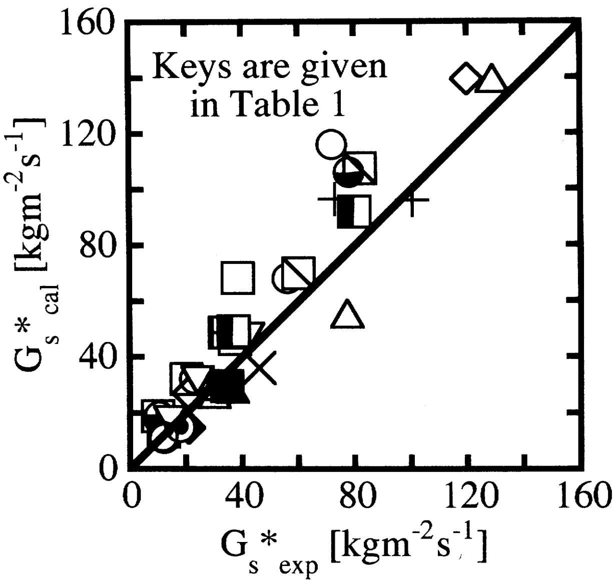

Fig. 8 Comparison between experimentally determined and calculated saturation carrying capacity of gas by Eq. (1)

All the above experimental results give strong support to the analysis of the present study. Therefore, we can conclude that the proposed approach to determine the saturation carrying capacity of gas is reasonable and practicable. To elucidate the variation of saturation carrying capacity of gas G_s* with gas velocity and gas-solid properties, experimental data available in the literature are shown in **Table 1**.

To obtain accurate SCC data, more experimental data around G_s* are definitely helpful. In this study, however,the quite different variation trends of ε_{sd} with G_s in the range of $G_s < G_s$* and of $G_s > G_s$* have made it possible to determine G_s* with an acceptable accuracy for the existing experimental data, although there is some scattering around G_s* sometimes. In such a way, the data of G_s* obtained from the literature for various particles are plotted against gas velocity in **Fig. 7**. It is clearly shown that the saturation carrying capacity of gas increases with increasing gas velocity. In order to find a dimensionless correlation that might give a unified representation of the data shown above, we tried several approaches and ended up with the following dimensionless empirical correlation.

$$\frac{G_s^* d_p}{\mu} = 0.125\, Fr^{1.85}\, Ar^{0.63} \left(\frac{\rho_p - \rho_g}{\rho_g}\right)^{-0.44} \quad (1)$$

with the Archimedes number defined by $Ar = d_p^3 \rho_g g(\rho_p - \rho_g)/\mu^2)$ ranging from 4.7 to 1019 and the Froude number defined by $Fr = U_g/(gd_p)^{0.5})$ ranging from 41 to 226. The ratio of densities $((\rho_p-\rho_g)/\rho_g)$ varied from 607 to 3607 in the correlation. The correlation coefficient for Eq. (1) is 0.94, and the relative deviation for calculation of G_s* is within 30%, as shown in **Fig. 8**. In view of the diversity of the experimental conditions and the difficulty in obtaining

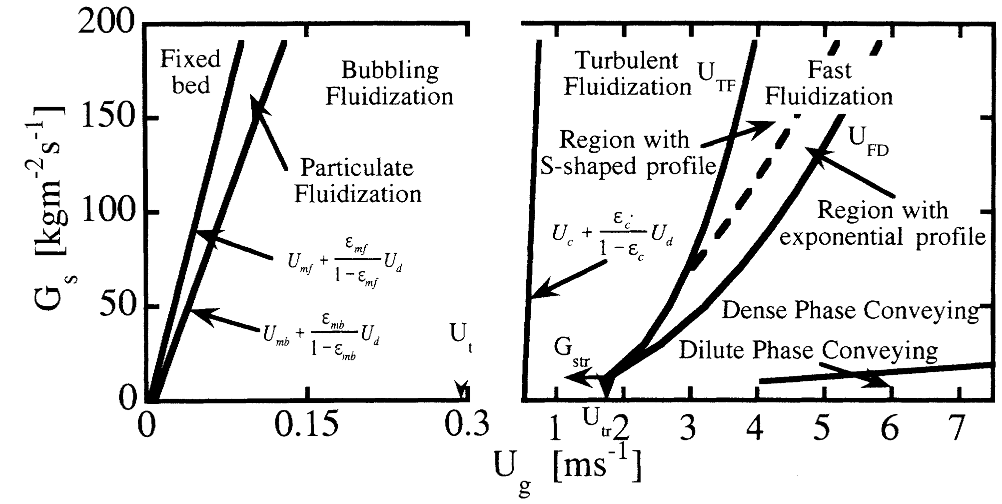

Fig. 9 A quantitative flow diagram showing the possible flow patterns involving a CFB for a typical group A powder (d_p = 60 μm, ρ_p = 1800kgm^{-3}, μ = 1.81 × 10^{-5} Pa. s, ρ_g = 1.25 kgm^{-3}, D = 0.2 m)

accurate SCC data, a deviation of this magnitude should be considered within experimental accuracy. It is worthwhile to point out that the proposed correlation is valid especially for group A particles of Geldart's classification to which most particles used in the present correlation belong.

3. Flow Patterns in CFBs

There have been a number of attempts over recent years to clarify the flow regimes appearing in a CFB (Takeuchi *et al.*, 1986, Yang and Sun, 1991). It has been long recognized that by the aid of a standpipe which allows particles to be returned to the bottom of the riser, a CFB can be operated at different regimes, varying from conventional fluidization (bubbling/slugging, turbulent) through a fast fluidization regime to pneumatic transport (Li and Kwauk, 1980, Yerushalmi and Cankurt, 1979, Takeuchi *et al.*, 1986, Bai *et al.*, 1993). Research indicated that the fast fluidization regime can be characterized by the non-uniformities of both radial and axial flow structures (Bai *et al.*, 1993, Li *et al.*, 1988, Takeuchi *et al.*, 1986). In the fast fluidization regime, either an S-shaped profile or a simple exponential profile in solid concentration is observed depending on the operating conditions (Bai *et al.*, 1993, Li and Kwauk, 1980). It is, however, uncertain under what conditions an S-shaped or simple exponential profile will occur within the fast fluidization regime.

The present study on SCC enables us to divide the fast fluidization into two regions, a region with S-shaped profile when $G_s \geq G_s$* and a region with exponential profile when $G_s < G_s$*. Extending the work of Bai *et al.* (1993), a quantitative flow diagram is presented in **Fig. 9** for a typical group A powder (d_p = 60 μm, ρ_p = 1800 kgm^{-3}) at the ambient condition (μ = 1.81 × 10^{-5}Pa.s, ρ_g = 1.25 kgm^{-3}). Transitions from the fixed bed, to particulate, to bubbling and to turbulent fluidization are estimated, based on the assumption that the slip velocity between gas and solids in the system with solid circulation is equal to that in the system without solid circulation. U_{mf}, U_{mb} and U_c under batch operation are calculated from the correlations of Wen & Yu (1966), Abrahamsen & Geldart (1980) and Cai *et al.*(1989), respectively. The transitions from fast fluidization to dense phase conveying and to dilute phase conveying are estimated, based on the generalized correlations proposed by Bai *et al.* (1993). The transport velocity U_{tr} and the corresponding solids circulation rate G_{str}, calculated by the correlations of Bai *et al.* (1993), represent the critical conditions under which there will occur a direct transition from turbulent fluidization to dense phase conveying and vice versa.

As shown in this figure, at a lower solid circulation rate, the axial flow pattern in fast fluidization may show only an exponential solid profile, while at high solid circulation rate the axial flow pattern is changed from an S-shaped profile to an exponential profile as the gas velocity is increased.

Conclusions

A generalized approach to determine the saturation carrying capacity of gas, G_s*, in high-velocity fluidized beds is discussed. In accordance with its physical interpretation, the saturation carrying capacity of gas was determined as the solid circulation rate at which a maximum achievable or saturation solid concentration in the dense region of the CFB is reached. Experiments demonstrated that the saturation carrying capacity of gas is a function of gas velocity and gas-solid properties, and a generalized correlation was therefore proposed on the basis of literature data. Finally, a quantitative flow diagram showing flow conditions for the existence of S-shaped and exponential profiles of solid holdup was presented.

Nomenclature

Ar	=	Archimedes number (= $d_p^3 \rho_g g (\rho_p - \rho_g)/\mu^2$)	[-]
D	=	riser diameter	[m]
D_s	=	standpipe diameter	[m]
d_p	=	particle diameter	[m]
Fr	=	Froude number (= $U_g/(g d_p)^{0.5}$)	[-]

G_s	=	solids circulation rate	[kgm^{-2}s^{-1})]
G_s*	=	solids saturation carrying capacity	[kgm^{-2}s^{-1})]
L_d	=	static bed height in the standpipe	[m]
U_c	=	transition velocity from bubbling to turbulent fluidization	[ms^{-1}]
U_d	=	superficial solid velocity (= G_s/ρ_p)	[ms^{-1}]
U_g	=	superficial gas velocity	[ms^{-1}]
U_{mb}	=	minimum bubbling fluidization velocity	[ms^{-1}]
U_{mf}	=	minimum fluidization velocity	[ms^{-1}]
U_t	=	particle terminal velocity	[ms^{-1}]
ρ_g	=	gas density	[kgm^{-3}]
ρ_p	=	particle density	[kgm^{-3}]
μ	=	gas viscosity	[Pa.s]
ε_{sd}	=	average solid holdup at the bottom of the riser.	[-]

Literature Cited

1) Abrahamsen, A. R. and D. Geldart; "Behavior of Gas-Fluidized Beds of Fine Powders. Part I. Homogenous Expansion," *Powder Technology*, **26**, 35-46 (1980)
2) Bai, D., Y. Jin and Z.-Q. Yu; "Flow Regimes in Circulating Fluidized Beds," *Chem. Eng. Technol.*, **16**, 307-313 (1993)
3) Bai, D., Y. Jin, Z.Yu and J. Zhu; "The Axial Distribution of the Cross-Sectionally Averaged Voidage in Fast Fluidized Beds," *Powder Technology*, **71**, 51-58 (1992)
4) Bai, D. and K. Kato; "Quantitative Estimation of Solids Holdups at the Dense and Dilute Regions of Circulating Fluidized Beds," submitted to *Powder Technology*, 1994
5) Bi, H.-T., P.-J. Jiang, R.-J. Jean and L.-S. Fan; "Coarse-Particle Effects in a Multisolid Circulating Fluidized Bed for Catalytic Reactions," *Chem. Eng. Sci.*, **47**, 3113-3124 (1992)
6) Bi, H. T., Y. Jin, Z.-Q. Yu and D. Bai; "The Radial Distribution of Heat Transfer Coefficient in Fast Fluidized Bed," *Fluidization VI*, pp.702-708, Engineering Foundation, New York (1989)
7) Cai, P., S. P. Chen, Y. Jin, Z.-Q. Yu and Z.-W. Wang; "Effect of Temperature and Pressure on the Transition from Bubbling to Turbulent Fluidization," *AIChE Symp. Ser.*, **85**, 34-43 (1989)
8) Chang, H. and M. Louge; "Fluid Dynamic Similarity of Circulating Fluidized Beds," *Powder Technology*, **70**, 259-270 (1992)
9) Chen, B., Y. Li, F. Wang, S. Wang and M. Kwauk; "Study on Fast Fluidization," *Chem. Metallurgy* (in Chinese), (4), 20-28 (1980)
10) Gao, S; "Solid Circulation Rate and Axial Voidage Distribution in Fast Fluidized Bed, " *Master theses*, Shenyang Research Institute of Chem. Eng., China (1990)
11) Kunii, D. and O. Levenspiel; Fluidization Engineering, 2nd ed., Butterworth-Heinmann, Boston, USA (1991)
12) Li, J., Y. Tung and M. Kwauk; "Axial Voidage Profiles of Fast Fluidized Beds in Different Operating Regions," *Circulating Fluidized Bed Technology II*, pp.193-203, Pergamon Press, Oxford (1988)
13) Li Y. and M. Kwauk; "The Dynamics of Fast Fluidization," *Fluidization*, pp.537-541, Plenum Press, New York (1980)
14) Matsen, T. M.; "Mechanisms of Choking and Entrainment," *Powder Technology*, **32**, 21-33 (1982)
15) Nishino, K; "Solids Holdup in Fast Fluidized Beds," *Master theses*, Gunma University, Japan (1990)
16) Ouyang, S. and O. E. Potter; "Consistency of Circulating Fluidized Bed Experimental Data," *Ind. Eng. Chem. Res.*, **32**, 1041-1045 (1993)
17) Rhodes, M. J. and D. Geldart; "The Hydrodynamics of Recirculating Fluidized Beds," *Circulating Fluidized Bed Technology*, pp.193-200, Pergamon Press, New York(1986)
18) Takeuchi, H., T. Hirama, T. Chiba, J. Biswas and L. S. Leung; "A Quantitative Definition and Flow Regime Diagram for Fast Fluidization," *Powder Technology*, **47**, 195-199(1986)
19) Weinstein, H., R. A. Graff, M. Meller and M. Shao; "The Influence of the Imposed Pressure Drop Across a Fast Fluidized Bed," *Fluidization*, pp.299-306, Engineering Foundation, New York(1984)
20) Wen, C. Y. and Y. H. Yu; "A Generalized Method for Predicting the Minimum Fluidization Velocity," *AIChE J.*, **12**, 610-617(1966)
21) Wen, C. Y. and L. H. Chen; "Fluidized Bed Freeboard Phenomena: Entrainment and Elutriation," *AIChE J.*, **28**, 117-128(1982)
22) Yang, G.-L and J.-K. Sun; "Transition of Flow Regime from Turbulent to Fast Fluidization and from Fast to Dilute Phase Transport," *Fluidization'91, Science and Technology*, pp.37-45, Science Press, Beijing(1991)
23) Yang, W. C.; "Criteria for Choking in Vertical Pneumatic Conveying Line," *Powder Technology*, **35**, 143-150(1983)
24) Yerushalmi, J. and N. T. Cankurt; "Further Studies of Regimes of Fluidization," *Powder Technology*, **24**, 187-295(1979)
25) Yerushalmi, J. and A. Avidan, "High Velocity Fluidization," *Fluidization*, 2nd ed., pp.225-289, Academic Press, London(1985)
26) Zenz, F. A. and N. A. Weil; "A Theoretical-Empirical Approach to the Mechanism of particle Entrainment from Fluidized Beds," *AIChE J.*, **4**, 472-479(1958)
27) Zenz, F. A. and D. F. Othmer; *Fluidization and Fluid-Particle Systems*, Reinhold Publishing Co., New York (1960)